Articles

Glutamate 189 of the D1 Polypeptide Modulates the Magnetic and Redox Properties of the Manganese Cluster and Tyrosine Y_Z in Photosystem II†

Richard J. Debus,*,‡ Kristy A. Campbell,§ Donna P. Pham,‡ Anna-Maria A. Hays,‡ and R. David Britt*,§

Department of Biochemistry, University of California, Riverside, California 92521-0129, and Department of Chemistry, University of California, Davis, California 95616

Received November 30, 1999; Revised Manuscript Received March 28, 2000

ABSTRACT: Recent models for water oxidation in photosystem II postulate that the tyrosine Y_Z radical, $Y_Z^{\bullet}$, abstracts both an electron and a proton from the Mn cluster during one or more steps in the catalytic cycle. This coupling of proton- and electron-transfer events is postulated to provide the necessary driving force for oxidizing the Mn cluster in its higher oxidation states. The formation of $Y_Z^{\bullet}$ requires the deprotonation of Y_Z by His190 of the D1 polypeptide. For $Y_Z^{\bullet}$ to abstract both an electron and a proton from the Mn cluster, the proton abstracted from Y_Z must be transferred rapidly from D1-His190 to the lumenal surface via one or more proton-transfer pathways. The proton acceptor for D1-His190 has been proposed to be either Glu189 of the D1 polypeptide or a group positioned by this residue. To further define the role of D1-Glu189, 17 D1-Glu189 mutations were constructed in the cyanobacterium *Synechocystis* sp. PCC 6803. Several of these mutants are of particular interest because they appear to assemble Mn clusters in 70−80% of reaction centers in vivo, but evolve no O_2. The EPR and electron-transfer properties of PSII particles isolated from the D1-E189Q, D1-E189L, D1-E189D, D1-E189N, D1-E189H, D1-E189G, and D1-E189S mutants were examined. Intact PSII particles isolated from mutants that evolved no O_2 also exhibited no S_1 or S_2 state multiline EPR signals and were unable to advance beyond an altered $Y_Z^{\bullet}S_2$ state, as shown by the accumulation of narrow "split" EPR signals under multiple turnover conditions. In the D1-E189G and D1-E189S mutants, the quantum yield for oxidizing the S_1 state Mn cluster was very low, corresponding to a ≥1400-fold slowing of the rate of Mn oxidation by $Y_Z^{\bullet}$. In Mn-depleted D1-Glu189 mutant PSII particles, charge recombination between $Q_A^{\bullet-}$ and $Y_Z^{\bullet}$ in the mutants was accelerated, showing that the mutations alter the redox properties of Y_Z in addition to those of the Mn cluster. These results are consistent with D1-Glu189 participating in a network of hydrogen bonds that modulates the properties of both Y_Z and the Mn cluster and are consistent with proposals that D1-Glu189 positions a group that accepts a proton from D1-His190.

Photosynthetic water oxidation takes place in photosystem II (PSII)[1] near the lumenal surface of the thylakoid membrane. PSII is a multisubunit, integral membrane protein complex (*1*−*3*) that utilizes light energy to oxidize water and reduce plastoquinone [for review, see (*4*−*11*)]. The oxygen-evolving catalytic site contains four Mn ions that are arranged as a magnetically coupled tetramer (*12*, *13*) [reviewed in (*14*)]. This tetrameric Mn cluster accumulates oxidizing equivalents in response to photochemical events within PSII, and then catalyzes the oxidation of two water molecules, releasing one molecule of O_2 as a byproduct. The photochemical events that precede water oxidation take place in a heterodimer of two homologous polypeptides known as D1 and D2. These events are initiated by the capture of light by an antenna complex that is located peripherally to PSII. The excitation energy is transferred to the photochemically active chlorophyll species known as P_{680}. Excitation of P_{680} results in formation of the charge-separated state, $P_{680}^{\bullet+}Pheo^{\bullet-}$, where Pheo is a molecule of pheophytin. The $Pheo^{\bullet-}$ radical rapidly reduces Q_A (a molecule of plastoquinone), forming

† This work was supported by the National Institutes of Health (GM43496 to R.J.D. and GM48242 to R.D.B.) and by the National Science Foundation (MCB 9513648 to R.D.B.).

* To whom correspondence should be addressed. R.J.D.: Phone (909) 787-3483, Fax (909) 787-4434, E-mail debusrj@citrus.ucr.edu. R.D.B.: Phone (530) 752-6377, Fax (530) 752-8995, Email: rdbritt@ucdavis.edu.

‡ University of California, Riverside.

§ University of California, Davis.

[1] Abbreviations: Chl, chlorophyll *a*; Car, carotenoid; Chl_Z, monomeric Chl species that is oxidized by $P_{680}^{\bullet+}$, probably via a molecule of carotenoid; cyt, cytochrome *c*; DCMU, 3-(3,4-dichlorophenyl)-1,1-dimethylurea; DMSO, dimethyl sulfoxide; EPR, electron paramagnetic resonance; ENDOR, electron nuclear double resonance; fwhm, full width at half-maximum; Pheo, pheophytin; PSII, photosystem II; PPBQ, phenyl-1,4-benzoquinone; P_{680}, chlorophyll species that serves as the light-induced electron donor in PSII; Y_Z, tyrosine residue that mediates electron transfer between the Mn cluster and $P_{680}^{\bullet+}$; Y_D, tyrosine residue that acts as an alternate electron donor to $P_{680}^{\bullet+}$; Q_A, primary plastoquinone electron acceptor; MES, 2-(*N*-morpholino)ethanesulfonic acid; wild-type*, control strain of *Synechocystis* sp. PCC 6803 constructed in identical fashion as the D1-Glu189 mutants, but containing the wild-type *psb*A-2 gene.

10.1021/bi992749w CCC: $19.00 © 2000 American Chemical Society
Published on Web 05/06/2000

the anionic radical, $Q_A^{\bullet -}$. The $P_{680}^{\bullet +}$ radical rapidly oxidizes tyrosine Y_Z (Tyr161 of the D1 polypeptide), forming the neutral radical, $Y_Z^{\bullet}$. This radical in turn oxidizes the Mn cluster, while $Q_A^{\bullet -}$ reduces the secondary plastoquinone, Q_B. Subsequent charge-separations result in further oxidation of the Mn cluster. During each catalytic cycle, the Mn cluster cycles through five oxidation states termed S_n, where *n* denotes the number of oxidizing equivalents stored. The S_1 state predominates in dark-adapted samples. The S_3 state may have one oxidizing equiv localized on a Mn ligand: whether Mn is oxidized during the $S_2 \rightarrow S_3$ transition is currently under debate [e.g., see (*15*) versus (*16*)]. The S_4 state is a transient intermediate that reverts to the S_0 state with the concomitant release of O_2.

Simulations of EPR and ENDOR data obtained with samples trapped in the $S_2Y_Z^{\bullet}$ state show that the point−dipole distance between $Y_Z^{\bullet}$ and the Mn cluster is 7−9 Å (*13*, *17*−*20*) [also see (*21*, *22*)]. This point−dipole distance is compatible with direct hydrogen bonding between Y_Z and Mn-bound substrate water molecules (*10*, *23*, *24*) but is equally compatible with indirect hydrogen bonding, such as via an intervening water molecule (*14*). Such hydrogen bonding, whether direct or indirect, is compatible with recent models for water oxidation that invoke proton-coupled electron transfer from Mn-bound substrate water molecules or water-derived Mn ligands to $Y_Z^{\bullet}$. In these models, $Y_Z^{\bullet}$ abstracts both an electron and a proton from the Mn cluster during some (*5*, *14*, *24*−*27*) or all (*23*, *28*−*33*) of the S state transitions. This coupling of proton- and electron-transfer events is postulated to provide the necessary driving force for oxidizing the Mn cluster in its higher S states.

Two residues postulated to have key roles in these models are His190 and Glu189 of the D1 polypeptide. The oxidation of Y_Z requires its deprotonation by a nearby base. This base has been identified as D1-His190 on the basis of site-directed mutagenesis (*34*−*41*) and chemical complementation (*39*, *41*) studies. For $Y_Z^{\bullet}$ to abstract both an electron and a proton from the Mn cluster during an S state transition, the proton abstracted from Y_Z must be transferred rapidly from D1-His190 to the lumenal surface. This transfer presumably occurs via a concerted "bucket brigade" or "domino" proton hopping (Grotthus) mechanism (*42*, *43*) within one or more proton-transfer pathways consisting of hydrogen-bonded amino acid residues and water molecules. Such pathways have been observed in the high-resolution structures of bacterial reaction centers (*44*, *45*), bacteriorhodopsin (*46*−*48*), cytochrome *f* (*49*, *50*), and cytochrome *c* oxidase (*51*−*53*). In PSII, one or more such pathways have been proposed to extend from D1-His190 to the lumenal surface and to involve D1-Glu189 (*29*, *31*, *33*). On the basis of a site-directed mutagenesis study, we previously proposed that D1-Glu189 participates in a network of hydrogen bonds that positions a group participating in proton release (*37*). More recently, this residue has been postulated to accept a proton from D1-His190 either directly or by positioning a water molecule or other group that acts as the proton acceptor (*29*, *31*, *33*). Several authors have proposed that a hydrogen bond connects D1-Glu189 and D1-His190 (*29*, *31*, *33*, *54*, *55*). Such a hydrogen bond would be consistent with structural simulations that place D1-Glu189 between Y_Z and the lumen (*56*−*59*).

To further define the role of D1-Glu189 in determining the properties of Y_Z and the Mn cluster, we have replaced this residue with Gln, Asp, Asn, His, Ser, Thr, Ala, Gly, Cys, Lys, Arg, Leu, Ile, Val, Met, Phe, and Tyr in the cyanobacterium *Synechocystis* sp. PCC 6803 (*37*, *60*). Only the Gln, Lys, Arg, Leu, and Ile mutations support photoautotrophic growth in *Synechocystis* strains that contain PSI. Several of the mutants are of particular interest because they appear to assemble Mn clusters in 70−80% of reaction centers in vivo, but evolve no O_2 [(*37*) and this study]. In this study, we present a characterization of PSII particles isolated from the Gln, Asp, Asn, His, Gly, Ser, and Leu mutants. We show that mutations of D1-Glu189 that abolish photoautotrophic growth and O_2 evolution also alter the redox properties of both the Mn cluster and Y_Z and perturb the magnetic properties of the Mn cluster. A preliminary account of this study has been presented (*60*).

MATERIALS AND METHODS

Construction of Site-Directed Mutants. The D1-Glu189 mutations were constructed in the *psbA-2* gene of the cyanobacterium *Synechocystis* sp. PCC 6803, as described previously (*61*). Plasmids bearing the D1-Glu189 mutations were transformed into *Synechocystis* strains that contain (*62*) or lack (*63*) PSI and *apc*E function. The control wild-type* strains containing and lacking PSI were constructed in identical fashion as the mutants except that the transforming plasmid carried no site-directed mutation. The designation "wild-type*" differentiates these strains from the native wild-type strain that contains all three *psb*A genes and is sensitive to antibiotics. Wild-type* and mutant cells containing PSI were propagated in the presence of 5 mM glucose (*64*) as described previously (*61*). Wild-type* and mutant cells lacking PSI were propagated in the presence of 15 mM glucose (*65*) as described previously (*39*).

Isolation of PSII Particles. Wild-type* and mutant PSII particles from cells containing PSI were isolated as described by Tang and Diner (*66*) with minor modification (*39*). Wild-type* and mutant PSII particles from cells lacking PSI were isolated as described previously (*39*) except that the detergent-extracted thylakoid membranes were applied to a 300 mL DEAE-Toyopearl 650s column, the column was washed with purification buffer [25% (v/v) glycerol, 50 mM MES−NaOH, 20 mM $CaCl_2$, 5 mM $MgCl_2$, 0.03% *n*-dodecyl β-D-maltoside, pH 6.0], and the purified PSII particles were eluted with purification buffer containing 30−50 mM $MgSO_4$. The O_2 evolution activity of the wild-type* PSII particles was 5−6 mmol of O_2 (mg of Chl)$^{-1}$ h^{-1}. For Mn-depleted PSII particles, the extraction of Mn was performed with NH_2OH and EDTA as described previously (*39*). The residual O_2 evolution activity of the Mn-depleted wild-type* preparations was ≤5% in comparison to untreated wild-type* PSII particles. Purified PSII particles were concentrated to ≈0.5 mg of Chl/mL by ultrafiltration (*66*), frozen in liquid N_2, and stored at −80 °C. For EPR experiments, PSII particles were concentrated further with Centricon-100 concentrators (Millipore Corp., Bedford, MA).

EPR Measurements. EPR spectra were recorded with a Bruker ECS106 X-band CW-EPR spectrometer equipped with an ER-4116DM dual mode cavity. Cryogenic temperatures were obtained with an Oxford ESR900 liquid helium

cryostat. The temperature was controlled with an Oxford ITC503 temperature and gas flow controller that was equipped with a gold−iron chromel thermocouple. Samples were illuminated in a non-silvered dewar at 195 K (methanol/dry ice) or at approximately 273 K [above liquid N_2 (*67*)] using a focused 300 W IR-filtered Radiac light source and a Schott 150 W IR-filtered fiber optic lamp and were immediately frozen in liquid N_2 after illumination.

Optical Measurements. Transient absorbance changes of Y_Z at 287.5 nm ($\Delta A_{287.5}$) and Q_A at 325 nm (ΔA_{325}) were measured with a modified CARY-14 spectrophotometer (On-Line Instrument Systems, Inc., Bogart, GA) operated in the single-beam mode (*39*). The photomultiplier tube was protected by two Corion Solar Blind filters. Actinic flashes (approximately 4 μs fwhm) were provided by a Xenon Corp. (Woburn, MA) model 457A xenon flash-lamp system (0.5 μF capacitor charged to 7−8 kV). The flashes were passed through two 2-mm-thick Schott WG-360 filters, two 2-mm-thick Schott RG-610 filters, and one Corion LS-750 filter and were directed to the sample cuvette with a 3.8-m-long flexible light guide (Schott Fiber Optics, Southbridge, MA). The cuvette containing the sample was held in a thermostated jacket. For measurements, samples were diluted (10 μg of Chl into 0.5 mL final volume) into purification buffer containing 0.03% *n*-dodecyl β-D-maltoside. To ensure the oxidation of Q_A and Y_D prior to data acquisition, the following procedures were employed. For measurements at 325 nm, samples were incubated in the presence of 10 μM $K_3Fe(CN)_6$ for 2 min, and then given 6 flashes 20 s apart and dark-adapted for another 2 min before DCMU (dissolved in DMSO) was added to 25 μM. The samples were then subjected to 28 flashes spaced 1 min apart. Data acquisition commenced with the fourth flash. For measurements at 287.5 nm, samples were incubated in the presence of 10 μM $K_3Fe(CN)_6$ for 2 min, and then given 154 flashes spaced 10 s apart. Data acquisition commenced with the 11th flash. Kinetics were analyzed with Jandel Scientific's (San Rafael, CA) PeakFit program, version 4.0.

Other Procedures. Measurements of chlorophyll *a* fluorescence in intact cells were performed with a modified Walz (Effeltrich, Germany) pulse-amplitude-modulated fluorometer, as described previously (*37*, *61*). The relative PSII content of cells on a chlorophyll basis was estimated from the total yield of variable chlorophyll *a* fluorescence measured in the presence of DCMU and hydroxylamine (*37*, *61*). Chlorophyll *a* concentrations were determined, after extraction into methanol, with an extinction coefficient of 79.24 $(mg/mL)^{-1}$ cm^{-1} at 665.2 nm (*68*), as described previously (*61*). Light-saturated rates of oxygen evolution in intact cells and isolated PSII particles were measured at 25.0 °C as described previously (*39*, *61*). For PSII particles, each sample contained 5 μg of Chl in 1.6 mL of 1 M sucrose, 50 mM MES−NaOH, pH 6.5, 25 mM $CaCl_2$, 10 mM NaCl, 0.4 mM 2,6-dichloro-*p*-benzoquinone (purified by sublimation), and 1 mM potassium ferricyanide. Illumination was provided by two Dolan-Jenner (Woburn, MA) model 180 fiber optics illuminators equipped with EJV bulbs. The light was passed through Dolan-Jenner infrared and red cutoff filters and directed to both sides of the sample with Dolan-Jenner fiber optic light guides. The Clark-type electrode was calibrated with hydrogen peroxide [freshly opened J. T. Baker ULTREX grade (Phillipsburg, NJ)] and catalase (*69*).

Table 1: Comparison of Wild-Type* and D1-Glu189 Mutant Strains in Vivo[a]

strain	photoautotrophic growth[b]	O_2 evolution[c] (% of wt*)	app PSII content[d] (% of wt*)	fraction of centers with photooxidizable Mn ions (%)[e]
wild-type*	+	100	100	100
E189Q[f]	+	67 ± 5	95 ± 12	87 ± 3
E189K	+	83 ± 7	73 ± 6	89 ± 3
E189R	+	70 ± 6	66 ± 2	88 ± 4
E189L	+	37 ± 5	55 ± 5	73 ± 7
E189I	+	62 ± 5	60 ± 5	88 ± 4
E189D[f]	−	<5	108 ± 6	87 ± 3
E189N[f]	−	6 ± 2	121 ± 6	87 ± 3
E189H	−	<5	104 ± 12	75 ± 2
E189G	−	<5	112 ± 5	75 ± 3
E189A	−	<5	95 ± 3	30 ± 10
E189S	−	<5	108 ± 8	69 ± 6
E189T	−	<5	90 ± 12	37 ± 6
E189V	−	<5	72 ± 18	72 ± 3
E189M	−	<5	109 ± 8	44 ± 3
E189C	−	<5	70 ± 9	71 ± 3
E189Y	−	<5	54 ± 10	46 ± 4
E189F	−	<5	70 ± 7	56 ± 2

[a] Data acquired with cells containing PSI. [b] Measured in growth medium without glucose. [c] Initial rates measured in growth medium. The light-saturated rate of O_2 evolution in wild-type* cells was 680 ± 30 μmol of O_2 (mg of Chl)$^{-1}$ h^{-1}. [d] Estimated from the total yield of variable chlorophyll *a* fluorescence ($F_{max} - F_0$). [e] Estimated by comparing the fraction of $Q_A^{\bullet -}$ photoaccumulated after 10−15 s of illumination in the presence of DCMU with that in wild-type* and D1-D170A cells (*37*, *61*). [f] Data from (*37*).

Measurements of O_2 evolution were conducted for 10 s commencing 10−15 s after the illuminators were switched on. Longer data collection times were not employed because the light-saturated rates of O_2 evolution in the mutants diminished appreciably after longer illumination times. When used for EPR samples, PPBQ was purified by sublimation.

RESULTS

Growth, Oxygen Evolution, and PSII Contents of Mutant Cells. Cells containing PSI and bearing the D1-E189Q, D1-E189K, or D1-E189R mutations were photoautotrophic and evolved O_2 at 70−80% the rate of wild-type* cells (Table 1). The PSII contents of these cells were 66−95% compared to wild-type*. Cells containing PSI and bearing the D1-E189L or D1-E189I mutations were also photoautotrophic and evolved O_2 at 40−60% the rate of wild-type* cells. The PSII contents of these cells were 55−60% compared to wild-type*. Cells containing PSI and bearing the D1-E189D, D1-E189N, D1-E189H, D1-E189G, D1-E189A, D1-E189S, D1-E189T, D1-E189V, D1-E189M, D1-E189C, D1-E189Y, or D1-E189F mutations were nonphotoautotrophic, requiring glucose for propagation (Table 1). None of these nonphotoautotrophic mutants evolved O_2 to a significant extent, although D1-E189N cells evolved O_2 at 6 ± 2% the rate of wild-type* cells (*37*). The PSII contents of the nonphotoautotrophic mutants were ≥90% compared to wild-type*, except for the D1-E189V, D1-E189C, D1-E189Y, and D1-E189F mutants, whose PSII contents were 50−70% compared to wild-type*.

Fluorescence Characteristics of Mutant Cells. The fluorescence yield of cyanobacteria and chloroplasts arises primarily from PSII and is governed by the redox states of P_{680} and Q_A [for review, see (*70*−*72*)]. The fluorescence yield

of the state $P_{680}Q_A$ is low (F_0). The fluorescence yield of the state $P_{680}Q_A^{\bullet-}$ is 2−5-fold higher than F_0 because the rate constant of charge separation decreases in the presence of $Q_A^{\bullet-}$. The fluorescence yield of the state $P_{680}^{\bullet+}Q_A^{\bullet-}$ is low because $P_{680}^{\bullet+}$ is a fluorescence quencher. The different fluorescence yields of the states $P_{680}Q_A^{\bullet-}$ and $P_{680}^{\bullet+}Q_A^{\bullet-}$ form the basis of an assay that is sensitive either to the absence of photooxidizable Mn ions in PSII or to slow electron donation from the Mn cluster to $Y_Z^{\bullet}$ (*37*, *61*, *73*, *74*, *79*). This assay involves measuring the maximum yield of chlorophyll *a* fluorescence that follows each flash in a series of closely spaced saturating flashes. In wild-type* cells, the first saturating flash generates the highly fluorescent state $Y_Z^{\bullet}P_{680}Q_A^{\bullet-}$. The Mn cluster reduces $Y_Z^{\bullet}$ within 30−1300 μs [(*75*−*78*) and references cited therein], and the subsequent oxidation of $Q_A^{\bullet-}$ by Q_B generates the state $Y_ZP_{680}Q_AQ_B^{\bullet-}$, returning the fluorescence yield to F_0. The second saturating flash then regenerates the highly fluorescent state $Y_Z^{\bullet}P_{680}Q_A^{\bullet-}$. If the Mn cluster is absent, or if electron transfer from the Mn cluster to $Y_Z^{\bullet}$ is slowed considerably, then the state $Y_Z^{\bullet}P_{680}Q_A$ persists when the second saturating flash is applied. This flash then forms the low fluorescent state $Y_Z^{\bullet}P_{680}^{\bullet+}Q_A^{\bullet-}$. Because $Y_Z^{\bullet}$ cannot reduce $P_{680}^{\bullet+}$, the maximum fluorescence yield after the second saturating flash is quenched by $P_{680}^{\bullet+}$. In all of the photoautotrophic mutants (i.e., in D1-E189Q, D1-E189K, D1-E189R, D1-E189L, and D1-E189I cells), the maximal fluorescence yield was essentially the same after each flash (e.g., Figure 1A), implying that nearly all PSII reaction centers in these mutants contain photooxidizable Mn clusters in vivo. In all of the nonphotoautotrophic mutants, the maximum fluorescence yield after the second and subsequent flashes was quenched substantially (e.g., Figure 1B,C), implying either that the Mn cluster is absent or that electron donation from Mn to $Y_Z^{\bullet}$ is slowed substantially in these mutants during one or more of the S state transitions.

The percentage of reaction centers containing photooxidizable Mn ions in vivo can be estimated from the rate that $Q_A^{\bullet-}$ photoaccumulates when cells are illuminated for 1−15 s in the presence of DCMU (*37*, *61*, *79*). The basis for this assay is that alternate PSII electron donors {e.g., Y_D (*80*, *81*) or cytochrome *b*-559 (*80*, *82*, *83*) [the latter via Chl_Z (*84*, *85*) and/or Car (*86*, *87*)]} reduce $P_{680}^{\bullet+}$ with low quantum yields (*80*−*82*, *88*), forming the relatively stable states $cyt^{ox}Q_A^{\bullet-}$ and $Y_D^{\bullet}Q_A^{\bullet-}$. The rate of oxidation of these alternate electron donors correlates with the equilibrium concentration of $P_{680}^{\bullet+}$ (*80*−*82*, *88*). Consequently, these donors are oxidized more rapidly in reaction centers that lack photooxidizable Mn ions than in those that contain photooxidizable Mn ions (*82*, *88*). During continuous illumination in the presence of DCMU, the states $Y_Z^{\bullet}Q_A^{\bullet-}$ and $S_2Q_A^{\bullet-}$ form and recombine until relatively stable states such as $cyt^{ox}Q_A^{\bullet-}$ and $Y_D^{\bullet-}Q_A^{\bullet-}$ photoaccumulate. By comparing the rate that $Q_A^{\bullet-}$ photoaccumulates in mutant cells with that in wild-type* and D1-D170A cells,[2] the percentage of PSII reaction centers containing photooxidizable Mn ions in vivo can be estimated (*37*, *61*, *79*). On the basis of this assay, the percentages of PSII reaction centers containing photooxidizable Mn ions were estimated to be 80−90% in D1-E189Q, D1-E189K, D1-E189R, D1-E189I, D1-E189D, and D1-E189N cells, 70−80% in D1-E189L, D1-E189H, D1-E189G, D1-E189V, and D1-E189C cells, 50−70% in D1-E189S and D1-E189F cells, and 30−50% in D1-E189A, D1-E189T, D1-E189M, and D1-E189Y cells (Table 1).

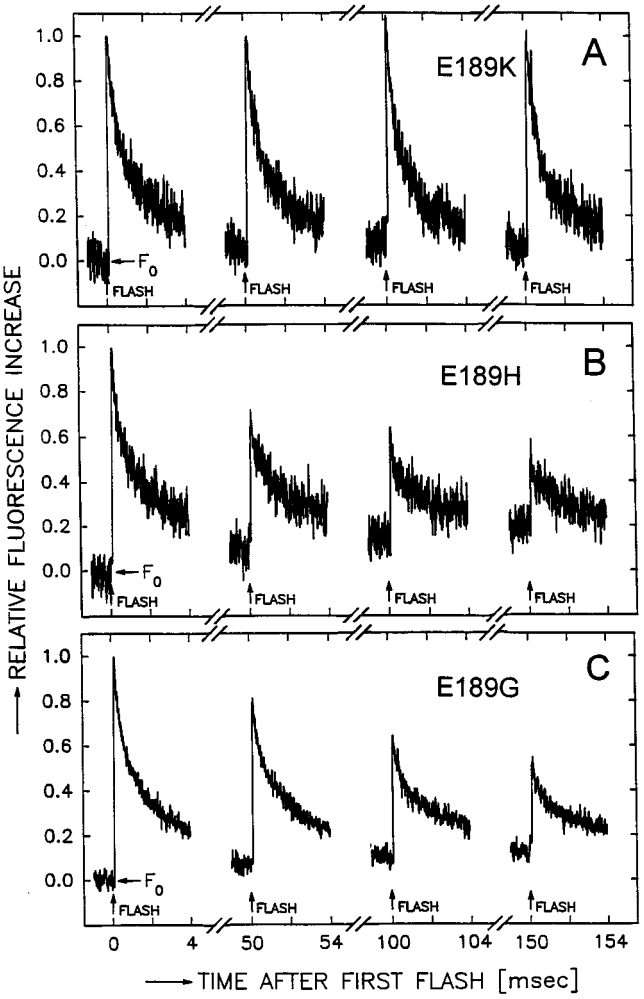

FIGURE 1: Yields of variable chlorophyll *a* fluorescence produced by each of four saturating flashes given at 50 ms intervals to D1-Glu189 mutant cells containing PSI. Five milliseconds of data are shown for each flash. (A) D1-E189K. (B) D1-E189H. (C) D1-E189G. Conditions: 20 μg of Chl in 0.58 mL of 50 mM MES−NaOH, 20 mM $CaCl_2$, and 10 mM NaCl, pH 6.5, 274 K. The cells were incubated in darkness for 1 min before the monitoring flashes were switched on. The frequency of the monitoring flashes was switched from 1.6 to 100 kHz for 5 ms beginning 1 ms before each saturating flash. The vertical scales are normalized to the maximum $(F - F_0)/F_0$ values measured after the first flash in each series. The data in (A) are representative for D1-Glu189 mutants that grow photoautotrophically. The data in (B) and (C) are representative for nonphotoautotrophic D1-Glu189 mutants, i.e., those that require glucose for propagation.

Oxidation of $Q_A^{\bullet-}$ by Mn or $Y_Z^{\bullet}$ in Intact and Mn-Depleted PSII Particles. To further define the role of D1-Glu189, PSII particles were isolated from the mutants D1-E189Q, D1-E189L, D1-E189D, D1-E189N, D1-E189H, D1-E189G, and D1-E189S. The O_2 evolution rates of the D1-E189Q and D1-E189L PSII particles were 2.4 ± 0.2 mmol of O_2 (mg of Chl)$^{-1}$ h^{-1} and 2.7 ± 0.2 mmol of O_2 (mg of Chl)$^{-1}$ h^{-1}, respectively, or 40−45% the rate of wild-type* PSII particles. To further characterize the Mn clusters in the mutant PSII particles, the kinetics of charge recombination between $Q_A^{\bullet-}$ and the donor side of PSII were measured after a single flash

[2] The PSII reaction centers of D1-D170A cells contain no photooxidizable Mn ions (*61*).

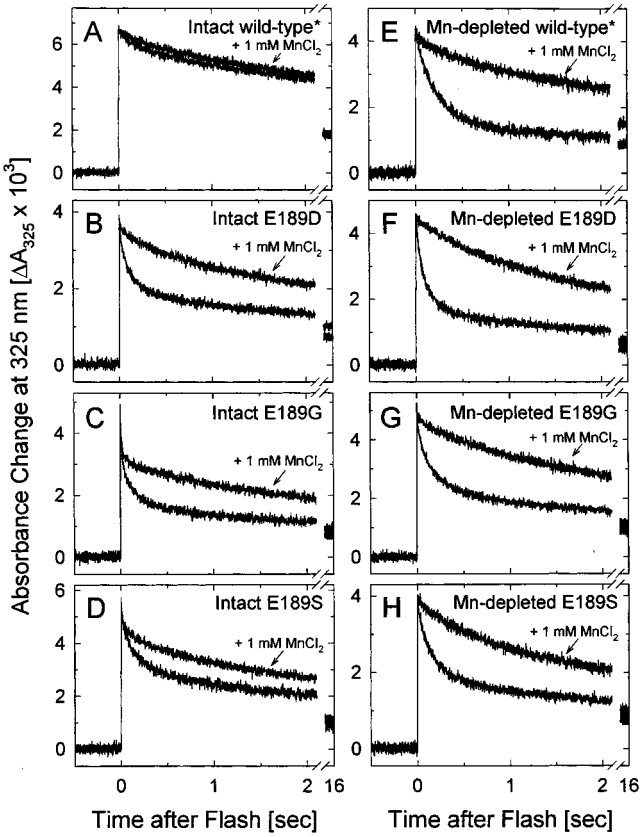

FIGURE 2: Formation and decay of $Q_A^{\bullet-}$ after a single flash applied to intact and Mn-depleted PSII particles in the absence and presence of 1.0 mM $MnCl_2$, as measured at 325 nm. (A) Intact wild-type* PSII particles. Note that the traces obtained in the absence and presence of 1.0 mM $MnCl_2$ nearly overlap. (B) Intact D1-E189D PSII particles. (C) Intact E189G PSII particles. (D) Intact D1-E189S PSII particles. (E) Mn-depleted wild-type* PSII particles. (F) Mn-depleted D1-E189D PSII particles. (G) Mn-depleted D1-E189G PSII particles. (H) Mn-depleted D1-E189S PSII particles. To facilitate comparisons, the amplitudes of the traces obtained in the presence of $MnCl_2$ were multiplied by factors of 1.28, 1.07, 1.19, 1.49, 1.04, 1.05, and 1.07 in panels B−H, respectively. Experimental conditions: 20 μg Chl/mL in 25% (v/v) glycerol, 50 mM MES−NaOH (pH 6.0), 20 mM $CaCl_2$, 5 mM $MgCl_2$, 0.03% *n*-dodecyl-β-D-maltoside, 10 μM $K_3Fe(CN)_6$, 25 μM DCMU, 1% DMSO, pH 6.0, 294 K. Traces obtained in the absence of added $MnCl_2$ in panels A−H represent the average of 25, 50, 50, 25, 25, 50, 50, and 50 sweeps, respectively. Traces obtained in the presence of 1.0 mM $MnCl_2$ in panels A−H represent the average of 25, 100, 50, 50, 50, 50, 50, and 50 sweeps, respectively. Samples were replaced after 25 sweeps.

(Figure 2). These measurements were conducted at 325 nm, a wavelength where interference from $Y_Z^{\bullet}$ and the Mn cluster is minimal (*89*−*93*). In both wild-type* and mutant particles, the $Q_A^{\bullet-}$ decay kinetics were fit with three exponentially decaying phases[3] (Table 2). The most rapidly decaying phase, with rate constant k_1, was assumed to represent charge recombination between $Q_A^{\bullet-}$ and $Y_Z^{\bullet}$ (*90*, *93*, *94*). This phase had $k_1^{-1} \approx 200$ ms in wild-type* PSII particles, $k_1^{-1} \approx 160$ ms in D1-E189Q, D1-E189N, and D1-E189H PSII particles, $k_1^{-1} \approx 140$ ms in D1-E189L PSII particles, $k_1^{-1} \approx 100$ ms in D1-E189D and D1-E189S PSII particles, and $k_1^{-1} \approx 50$ ms in D1-E189G PSII particles (Table 2). The percentage of reaction centers exhibiting k_1 was 11.4 ± 0.9% in intact wild-type* PSII particles (Figure 2A), 63 ± 1% in Mn-depleted wild-type* PSII particles (Figure 2E), ∼30% in D1-E189Q and D1-E189L PSII particles, ∼50% in D1-E189S, D1-E189D, D1-E189N, and D1-E189H PSII particles (e.g., Figure 2B,D), and ∼64% in D1-E189G PSII particles (Figure 2C).

In Mn-depleted PSII particles, a substantial percentage of reaction centers does not exhibit k_1; that is, a substantial percentage of $Q_A^{\bullet-}$ does not recombine with $Y_Z^{\bullet}$. The reason is that, in some Mn-depleted reaction centers, $P_{680}^{\bullet+}$ becomes reduced during the lifetime of $Y_Z^{\bullet}$ by an alternate electron donor [e.g., Y_D (*80*, *81*), Chl_Z (*84*, *85*), or Car (*86*, *87*)] because of the redox equilibrium, $Y_Z^{\bullet}P_{680} \leftrightarrow Y_ZP_{680}^{\bullet+}$ (*80*−*83*, *88*). The reduction of $P_{680}^{\bullet+}$ by an electron donor other than Y_Z generates the state $Y_ZQ_A^{\bullet-}$; the subsequent oxidation of $Q_A^{\bullet-}$ requires many seconds (*39*, *90*, *93*, *94*).

In intact wild-type* PSII particles, a significant percentage of reaction centers (11.4 ± 0.9%) exhibits k_1 (Table 2); that is, a significant percentage of $Q_A^{\bullet-}$ recombines with $Y_Z^{\bullet}$. In the presence of 0.1−1.0 mM $MnCl_2$, this percentage decreased to 7 ± 1% (not shown, but see Figure 2A). Exogenous Mn^{2+} ions rapidly reduce $Y_Z^{\bullet}$ in PSII particles that lack Mn clusters (*73*, *95*−*98*) (e.g., see Figure 2E−H), leaving $Q_A^{\bullet-}$ to be oxidized slowly, possibly by charge recombination with the Mn^{3+} ion that remains at the high-affinity Mn binding site (*99*). In Mn-depleted PSII particles from *Synechocystis* sp. PCC 6803, Mn^{2+} reduces $Y_Z^{\bullet}$ with $K_M = 1.5 \pm 0.5$ μM (*73*, *99*). Therefore, 0.1−1.0 mM $MnCl_2$ should eliminate k_1 in reaction centers that lack Mn clusters. However, because 7 ± 1% of intact wild-type* PSII particles continue to exhibit k_1 in the presence of 0.1−1.0 mM $MnCl_2$, a small percentage of $Q_A^{\bullet-}$ must recombine with $Y_Z^{\bullet}$ even when the high-affinity Mn binding site near Y_Z is occupied by a Mn cluster or by a Mn^{2+} ion. It is unlikely that this phenomenon is an artifact introduced during isolation of the PSII particles: when charge recombination between $Q_A^{\bullet-}$ and the donor side of PSII is measured in intact wild-type* cells of *Synechocystis* 6803, approximately 16% of the variable fluorescence yield decays[4] with $k_1^{-1} = 100 \pm 40$ ms (*61*) [also see (*73*)]. Heterogeneities or conformational equilibria that slow the reduction of $Y_Z^{\bullet}$ by Mn in a fraction of reaction centers may cause a small percentage of $Q_A^{\bullet-}$ to recombine with $Y_Z^{\bullet}$ despite the presence of a Mn cluster or a Mn^{2+} ion.[5]

To estimate the percentage of intact wild-type* PSII particles that contain flash-oxidizable Mn clusters, we assume that 0% of Mn-depleted PSII reaction centers contain flash-oxidizable Mn ions and that, in the presence of 1.0 mM $MnCl_2$, 100% of intact wild-type* PSII particles contain

[3] The exponentially decaying phases are reported in terms of initial amplitudes (% of total) and lifetimes (i.e., k^{-1}); that is, the time required for the amplitude to decay to 1/e of its initial value.

[4] At the pH values employed, all kinetic phases of charge recombination are more rapid in intact cells of *Synechocystis* sp. PCC 6803 than in isolated PSII particles (*73*, *101*).

[5] The microsecond phases of $P_{680}^{\bullet+}$ reduction in intact PSII preparations have also been proposed to reflect an equilibrium between different conformational states of PSII (*100*) or between different protonation states of hydrogen-bonded networks leading from Y_Z to the lumenal surface (*33*) [see also the discussion in (*41*)]. Such equilibria may contribute to photochemical misses in PSII by allowing $Q_A^{\bullet-}$ to reduce $P_{680}^{\bullet+}$ in the equilibrium population of reaction centers in which electron donation from Y_Z is slow (*100*). However, equilibria that slow the reduction of $Y_Z^{\bullet}$ by Mn in a small percentage of reaction centers probably would not contribute to photochemical misses in vivo because $Q_A^{\bullet-}$ would presumably be oxidized by Q_B before it could reduce $Y_Z^{\bullet}$.

Table 2: Kinetics of $Q_A^{\bullet-}$ Decay after a Flash in Intact and Mn-Depleted Wild-Type* and Mutant PSII Particles[a]

	k_1		k_2		k_3[b]		reaction centers with Mn clusters (%)
	%	k_1^{-1} (ms)	%	k_2^{-1} (s)	%	k_3^{-1} (s)	
wild-type*	11.4 ± 0.9	207 ± 34	38 ± 3	3.2 ± 0.4	51 ± 3	26 ± 3	92 ± 3[c]
Mn-depleted wild-type*	63 ± 1	190 ± 10	17 ± 1	1.6 ± 0.3	20 ± 1	>100	0[d]
E189Q	28 ± 4	160 ± 35	30 ± 4	2.7 ± 0.3	42 ± 5	43 ± 4	63 ± 4[e]
E189L	32 ± 3	143 ± 22	32 ± 1	2.0 ± 0.2	36 ± 2	34 ± 5	55 ± 6[e]
E189G	64 ± 1	54 ± 6	20 ± 1	1.9 ± 0.2	17 ± 1	>100	55 ± 4[f]
E1896+$MnCl_2$	38 ± 2	23 ± 1	37 ± 1	2.5 ± 0.2	25 ± 1	45 ± 7	55 ± 4[f]
E189S	48 ± 1	104 ± 13	27 ± 2	2.8 ± 0.2	25 ± 2	47 ± 10	63 ± 5[g]
E1895+$MnCl_2$	27 ± 2	65 ± 10	41 ± 1	2.8 ± 0.3	32 ± 2	41 ± 7	63 ± 5[f]
E189D	46 ± 1	108 ± 10	27 ± 2	2.4 ± 0.4	28 ± 3	44 ± 10	30 ± 3[e]
E189N	50 ± 2	160 ± 9	28 ± 1	2.3 ± 0.3	22 ± 2	>70	23 ± 4[e]
E189H	50 ± 1	161 ± 7	29 ± 1	1.8 ± 0.1	21 ± 2	>68	23 ± 3[e]

[a] Tabulated are the averages and sample standard deviations of 4−10 separate measurements conducted on each sample type. The exponentially decaying phases are reported in terms of initial amplitudes (% of total) and lifetimes (i.e., k^{-1}); that is, the time required for the amplitude to decay to 1/e of its initial value. [b] The values of k_3 should be considered approximate because only 16 s of data was subjected to the fitting procedure. [c] In the presence of 0.1−1.0 mM $MnCl_2$, % k_1 decreased to 7 ± 1% and 100% of wild-type* reaction centers were assumed to contain Mn clusters or Mn^{2+} ions (see text). [d] Assumed. [e] Calculated from the relation $100 \times [(63 - \% k_1)/(63 - 7)]$. [f] The percentage of E189G reaction centers containing Mn clusters that are photooxidized by a flash is $(63 - 64)/(63 - 7) = 0\%$. However, in $100 \times [(38 - 7)/(63 - 7)] = 55 \pm 4\%$ of E189G reaction centers, Mn clusters protect $Y_Z^{\bullet}$ from reduction by exogenous Mn^{2+} ions (see text). [g] The percentage of E189S reaction centers containing Mn clusters that are photooxidized by a flash is $(63 - 48)/(63 - 7) = 27 \pm 3\%$. In an additional $100 \times [(27 - 7)/(63 - 7)] = 36 \pm 4\%$ of E189S reaction centers, Mn clusters that are not photooxidized by a flash protect $Y_Z^{\bullet}$ from reduction by exogenous Mn^{2+} ions (see text).

flash-oxidizable Mn clusters or Mn^{2+} ions. Because 7 ± 1% of intact wild-type* PSII reaction centers exhibit k_1 in the presence of 0.1−1.0 mM $MnCl_2$ (see above) and 63 ± 1% of Mn-depleted wild-type* PSII reaction centers exhibit k_1 in the absence of added $MnCl_2$ (Table 2), the total dynamic range for % k_1 is (63 − 7)%. Therefore, because 11.4 ± 0.9% of intact wild-type* PSII reaction centers exhibit k_1 in the absence of added Mn^{2+} ions (Table 2), the percentage of intact wild-type* PSII reaction centers containing flash-oxidizable Mn clusters is $100 \times [(63 - 11.4)/(63 - 7)] = 92 \pm 3$.

To estimate the percentages of D1-Glu189 mutant PSII particles that contain flash-oxidizable Mn clusters, we proceed as in the previous paragraph, using the expression $100 \times (63 - \% k_1)/(63 - 7)$. In using this expression, we implicitly assume that the dynamic range for % k_1 is the same in D1-Glu189 mutant and wild-type* PSII particles. With this expression, the percentages of D1-Glu189 mutant PSII reaction centers containing flash-oxidizable Mn clusters are 63 ± 4% in D1-E189Q, 55 ± 6% in D1-E189L, 30 ± 3% in D1-E189D, 27 ± 3% in D1-E189S, 23 ± 4% in D1-E189N, and 23 ± 3% in D1-E189H PSII particles. No flash-oxidizable Mn clusters could be estimated with this analysis in D1-E189G PSII particles. However, the dynamic range for % k_1 may differ in these PSII particles because of the unusually rapid rate of charge recombination between $Q_A^{\bullet-}$ and $Y_Z^{\bullet}$ in intact D1-E189G PSII particles (Table 2).

To test the possibility that some of the D1-E189 mutant PSII particles contain more Mn clusters than are oxidized by a single flash, the kinetics of $Q_A^{\bullet-}$ oxidation were also measured in the presence of 1.0 mM $MnCl_2$. In the presence of 1.0 mM $MnCl_2$, the rate of $Q_A^{\bullet-}$ oxidation was slowed dramatically in all Mn-depleted PSII particles (Figure 2E−H) and in all intact D1-Glu189 mutant PSII particles [e.g., D1-E189D (Figure 2B)], with the exception of intact D1-E189G and D1-E189S PSII particles. In these PSII particles, 1.0 mM $MnCl_2$ slowed $Q_A^{\bullet-}$ oxidation only moderately (Figure 2C,D). In the presence of 1.0 mM $MnCl_2$, $Q_A^{\bullet-}$ was oxidized rapidly in 38 ± 2% of D1-E189G and 27 ± 2% of D1-E189S reaction centers, respectively (Table 2). Evidently, some D1-E189G and D1-E189S PSII particles contain Mn clusters that are not photooxidized by a flash but that protect $Y_Z^{\bullet}$ from reduction by exogenous Mn^{2+} ions. In this fraction of PSII particles, $Y_Z^{\bullet}$ is reduced by $Q_A^{\bullet-}$ rather than by exogenous Mn^{2+} ions. To estimate the percentages of these PSII particles in the D1-E189G and D1-E189S preparations, we proceed as in the previous paragraph, again assuming that the total dynamic range for % k_1 is (63 − 7)%. Therefore, the percentage of intact D1-E189G reaction centers containing Mn clusters that are not photooxidized by a flash but that protect $Y_Z^{\bullet}$ from reduction is $100 \times [(38 - 7)/(63 - 7)] = 55 \pm 4$. Therefore, at least 55 ± 4% of D1-E189G reaction centers contain Mn clusters (Table 2). The percentage of intact D1-E189S reaction centers containing Mn clusters that are not photooxidized by a flash is $100 \times [(27 - 7)/(63 - 7)] = 36 \pm 4$. Therefore, the total percentage of intact D1-E189S PSII particles containing Mn clusters is 63 ± 5% (i.e., 27 ± 3% plus 36 ± 4%). Of these, $100 \times (27/63) = 43 \pm 6\%$ reduce $Y_Z^{\bullet}$ after a flash and the remaining $100 \times (36/63) = 57 \pm 8\%$ protect $Y_Z^{\bullet}$ from reduction by Mn^{2+} ions.

Reduction of $Y_Z^{\bullet}$ by $Q_A^{\bullet-}$ in Mn-Depleted PSII Particles. In the absence of exogenous Mn^{2+} ions, the fastest phase of $Q_A^{\bullet-}$ oxidation, k_1, was more rapid in all D1-Glu189 mutant PSII particles than in wild-type* (Figure 2, Table 2). This observation suggests that charge recombination between $Q_A^{\bullet-}$ and $Y_Z^{\bullet}$ is accelerated in the D1-Glu189 mutants compared to wild-type*. However, the analysis is complicated by the presence of Mn clusters in some reaction centers but not others: the rate of charge recombination between $Q_A^{\bullet-}$ and $Y_Z^{\bullet}$ is determined by the rate of electron transfer from $Q_A^{\bullet-}$ to $P_{680}^{\bullet+}$ and by the equilibrium, $P_{680}^{\bullet+} Y_Z \leftrightarrow P_{680} Y_Z^{\bullet}$ (*74*, *80*−*82*, *88*, *93*). The equilibrium constant is greater in the absence of the Mn cluster [$K_{eq} = 90-120$ at pH 6.0 (*80*)] than in its presence [$K_{eq} = 20-30$ in the S_1 state (*102*, *103*)] because the midpoint potential of $Y_Z^{\bullet}/Y_Z$ decreases relative to that of $P_{680}^{\bullet+}/P_{680}$ in the absence of the Mn cluster (*80*, *93*, *103*, *104*). To eliminate this complication, the kinetics of $Y_Z^{\bullet}$ reduction were measured in wild-type* and D1-Glu189 mutant PSII particles after extraction of Mn. The

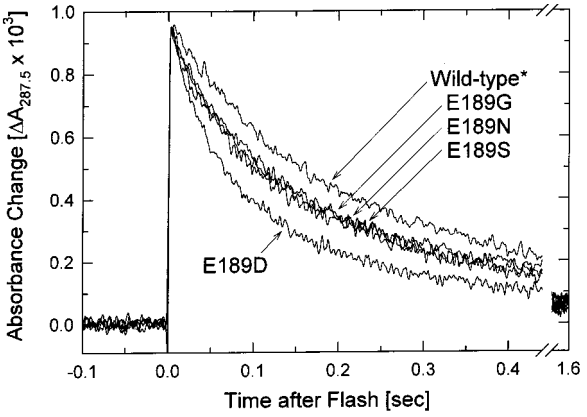

FIGURE 3: Formation and decay of $Y_Z^{\bullet}$ after a single flash applied to Mn-depleted PSII particles, as measured at 287.5 nm. Conditions: same as in Figure 4 but without DCMU or DMSO. Each trace represents the average of 432 sweeps. Samples were replaced after 144 sweeps.

kinetics were measured at 287.5 nm, an isosbestic point for $Q_A^{\bullet-}$ in *Synechocystis* sp. PCC 6803 (*60*, *93*), and were fit with two exponentially decaying phases (Figure 3). In Mn-depleted wild-type* PSII particles, 69 ± 5% of $Y_Z^{\bullet}$ decayed with $k^{-1} = 180 \pm 28$ ms, and the remainder decayed with $k^{-1} = 1.0 \pm 0.4$ s. In D1-E189G, D1-E189N, and D1-E189S PSII particles, ~80% of $Y_Z^{\bullet}$ decayed with $k^{-1} = 140-150$ ms, and the remainder decayed with $k^{-1} \approx 1.4$ s. In D1-E189D PSII particles, 85 ± 2% of $Y_Z^{\bullet}$ decayed with $k^{-1} = 104 \pm 9$ ms, and the remainder decayed with $k^{-1} = 1.2 \pm 0.3$ s. These data confirm that charge recombination between $Q_A^{\bullet-}$ and $Y_Z^{\bullet}$ is accelerated in D1-Glu189 mutant PSII particles in comparison to wild-type*.

EPR Spectra of D1-E189Q PSII Particles. A parallel polarization, integer spin multiline EPR signal was observed in dark-adapted D1-E189Q PSII particles (Figure 4, lower trace). This signal is similar to the S_1 state multiline EPR signal that is observed in wild-type* PSII particles from *Synechocystis* (Figure 4, upper trace) (*105*, *106*), and we assign it to the S_1 state in D1-E189Q PSII particles. A multiline EPR signal was also observed in the perpendicular mode after illumination of D1-E189Q PSII particles at 195 K (Figure 5, lower trace). This signal is similar to the S_2 state multiline EPR signal observed in wild-type* PSII particles illuminated under the same conditions (Figure 5, upper trace), and we assign it to the S_2 state in D1-E189Q PSII particles. After correcting for the different Chl contents of the two samples, the integrated area of the D1-E189Q S_2 state multiline EPR signal was approximately 64% of the integrated area of the wild-type* signal. Because 92 ± 3% of the wild-type* PSII reaction centers was estimated to contain photooxidizable Mn clusters (Table 2), we conclude that approximately 59% of the D1-E189Q PSII reaction centers gave rise to the S_2 state multiline EPR signal. A similar percentage (63 ± 4%) of D1-E189Q PSII particles was estimated to contain flash-oxidizable Mn clusters (Table 2). The percentages of PSII particles contributing to the S_1 state multiline signals were not estimated because of the presence of an underlying background signal that is observed in almost all parallel mode spectra of PSII. The shape of this background signal varies between samples, preventing accurate calculation of hyperfine signal areas. The S_1 and S_2 state multiline EPR signals of D1-E189Q PSII particles were the same whether the PSII particles were isolated from *Synechocystis* cells containing or lacking PSI.

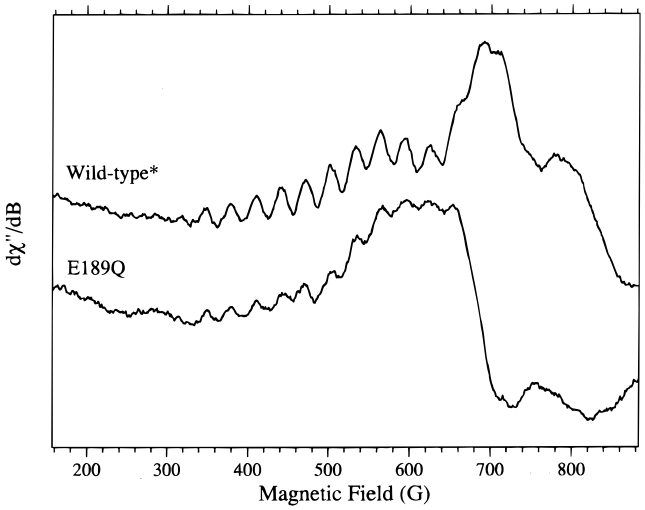

FIGURE 4: Parallel polarization EPR spectra of dark-adapted wild-type* (upper trace) and D1-E189Q (lower trace) PSII particles. After illumination, the samples used for Figure 5 (below) were dark-adapted for 1.5 h at 273 K before being flash-frozen in liquid N_2. Experimental conditions: dual mode cavity; microwave frequency, 9.42 GHz; microwave power, 51 mW; modulation amplitude, 8 G; modulation frequency, 100 kHz; time constant, 164 ms; conversion time, 164 ms; temperature, 2.7 K; 9 scans for wild-type* and 31 scans for D1-E189Q. The spectra have been normalized for Chl content and for the number of scans accumulated. Underlying the multiline features in each sample is an unidentified background signal that is observed in almost all parallel mode spectra of PSII. The shape of this background signal varies between samples, thus preventing a quantitative comparison of the integrated hyperfine signal intensity between the wild-type* and D1-E189Q mutant spectra.

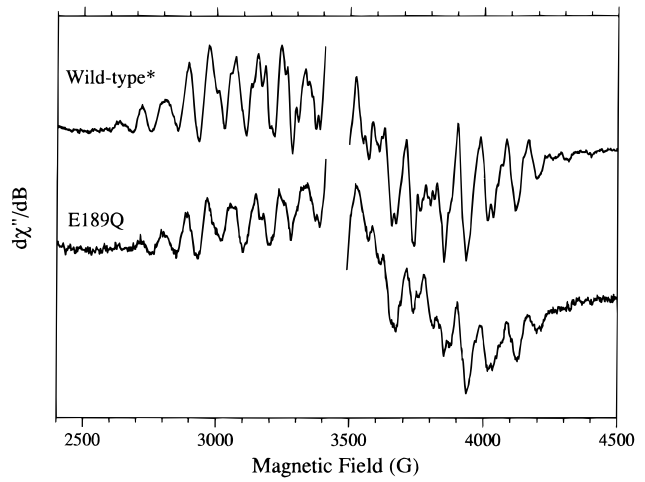

FIGURE 5: Light-*minus*-dark EPR spectra of wild-type* (upper trace) and D1-E189Q (lower trace) PSII particles. Samples were illuminated for 5 min at 195 K before being flash-frozen in liquid N_2. The wild-type* sample contained ~3.3 mg of Chl/mL and was isolated from cells lacking PSI. The D1-E189Q sample contained ~2.5 mg of Chl/mL, was isolated from cells containing PSI, and contained 1 mM DCMU and 1% DMSO. Sample buffer: 25% (v/v) glycerol, 50 mM MES−NaOH (pH 6.0), 20 mM $CaCl_2$, 5 mM $MgCl_2$, 25 mM $MgSO_4$, 0.03% *n*-dodecyl-*β*-D-maltoside. Experimental conditions: dual mode cavity; microwave frequency, 9.68 GHz; microwave power, 3.2 mW; modulation amplitude, 10 G; modulation frequency, 100 kHz; time constant, 20 ms; conversion time, 41 ms; temperature, 7 K; 60 scans. The spectra have been normalized for Chl content and have had the $g = 2.0$ region, containing the EPR signal of $Y_D^{\bullet}$, removed for clarity.

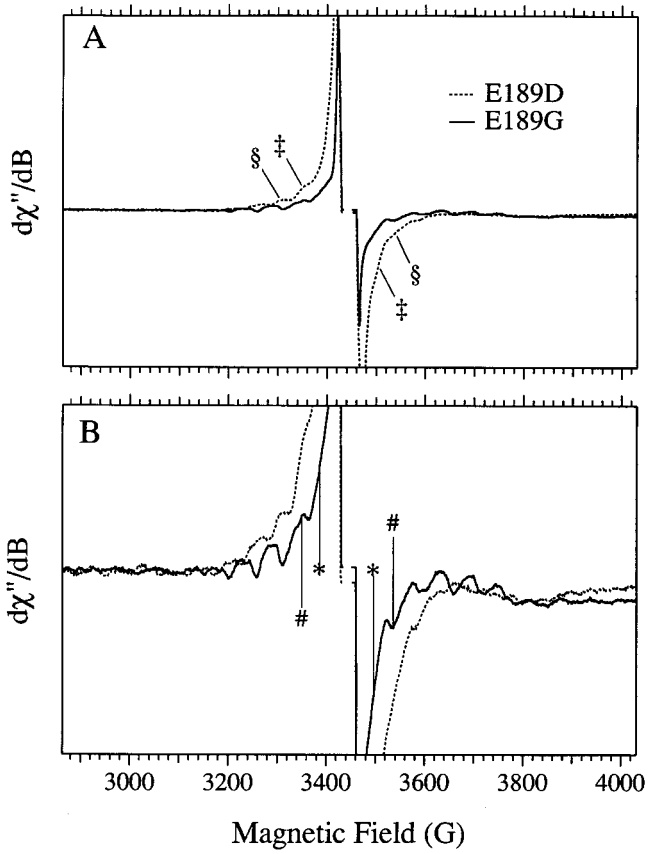

FIGURE 6: Light-*minus*-dark EPR spectra of the "split" EPR signal of D1-E189D and D1-E189G PSII particles. Samples [~4 mg of Chl/mL in 25% (v/v) glycerol, 50 mM MES−NaOH (pH 6.0), 20 mM $CaCl_2$, 5 mM $MgCl_2$, 30 mM $MgSO_4$, 0.03% *n*-dodecyl-*β*-D-maltoside, 0.6 mM $K_3Fe(CN)_6$, 0.6 mM PPBQ, 1% (v/v) DMSO] were illuminated for 28 s above liquid N_2 before being flash-frozen. The vertical scale of (B) is expanded relative to that in (A). The points marked by "‡" and "§" in the E189D spectrum are split by 155 and 235 G, respectively. The points marked by "∗" and "#" in the E189G spectrum are split by 110 and 185 G, respectively. Experimental conditions: dual mode cavity; microwave frequency, 9.68 GHz; microwave power, 3.2 mW; modulation amplitude, 10 G; modulation frequency, 100 kHz; time constant, 41 ms; conversion time, 82 ms; temperature, 7 K; 10 scans. The PSII particles were isolated from cells lacking PSI. The spectra have had the $g = 2.0$ region, containing the EPR signal of $Y_D^{\bullet}$, removed for clarity.

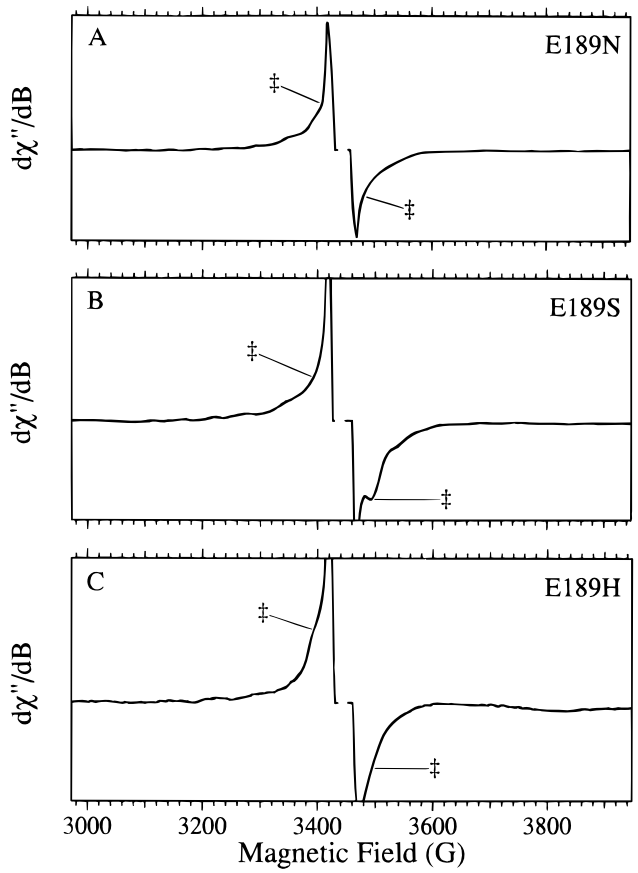

FIGURE 7: Light-*minus*-dark EPR spectra of the "split" EPR signal of (A) D1-E189N, (B) D1-E189S, and (C) D1-E189H PSII particles. The vertical scales differ from those in Figure 6. Samples [~6 mg of Chl/mL for (A), ~7 mg of Chl/mL for (B), and ~5 mg of Chl/mL for (C), in the same buffer as in Figure 3] were illuminated for 28 s above liquid N_2 before being flash-frozen. The points marked by "‡" are split by 75, 100, and 100 G in panels A, B, and C, respectively. Experimental conditions: dual mode cavity; microwave frequency, 9.68 GHz; microwave power, 3.2 mW; modulation amplitude, 10 G; modulation frequency, 100 kHz; time constant, 41 ms; conversion time, 82 ms; temperature, 7 K; 10 scans for (A) and (C), 7 scans for (B). The PSII particles were isolated from cells lacking PSI. The spectra have had the $g = 2.0$ region, containing the EPR signal of $Y_D^{\bullet}$, removed for clarity.

EPR Spectra of Non-O_2-Evolving PSII Particles. No S_1 state multiline EPR signal was observed in dark-adapted D1-E189D, D1-E189G, D1-E189N, D1-E189S, or D1-E189H PSII particles. Similarly, no S_2 state multiline EPR signal was observed in any of these PSII particles after illumination at 195 K or in D1-E189D or D1-E189G PSII particles after illumination at 273 K in the presence of DCMU (not shown).

Illumination of D1-E189D, D1-E189G, D1-E189N, D1-E189S, and D1-E189H PSII particles near 273 K in the presence of PPBQ and $K_3Fe(CN)_6$ as electron acceptors produced narrow "split" EPR signals (Figures 6 and 7). In D1-E189D PSII particles, the split signal had a line width of ~155 G and additional features split by ~235 G (Figure 6A). In D1-E189G PSII particles, the split signal had a line width of ~110 G (Figure 6B) plus additional features resembling the small flanking multiline peaks observed in acetate-treated PSII preparations from spinach (*13*, *17*−*20*, *107*−*111*). Hints of such flanking multiline peaks were also evident in the split signals observed in D1-E189N and D1-E189S PSII particles (Figure 7A,B). The split signals in D1-E189N, D1-E189S, and D1-E189H PSII particles had line widths of ~75, ~100, and ~100 G, respectively (Figure 7).

DISCUSSION

In this study, we show that mutations of D1-Glu189 that fail to support the photoautotrophic growth of cells containing PSI also alter the magnetic properties of the Mn cluster and perturb the redox properties of both the Mn cluster and Y_Z. On the basis of modeling studies (*56*−*59*), D1-Glu189 has been proposed to be a possible ligand of the Mn cluster. In cytochrome *c* from yeast, Lys can replace Met (*112*) and Arg can replace Met (*113*) and His (*114*, *115*) as ligands to Fe. In cytochrome *c*-550 from *Thiobacillus versutus*, Lys can replace Met as a ligand to Fe (*116*). In cytochrome *c* peroxidase, Gln can replace His as a ligand to Fe with little change in the enzyme's steady-state k_{cat} value (*117*). Consequently, the retention of O_2 evolution and photoautotrophic growth in the D1-E189Q, D1-E189K, and D1-E189R mutants would be consistent with ligation of the Mn cluster by D1-Glu189 if residues such as Asp, Asn, Ser, and Gly

are too small or inflexible to substitute.[6] However, in most of the nonphotoautotrophic D1-Glu189 mutants, more than 70% of the PSII reaction centers contain photooxidizable Mn clusters in vivo [(*37*) and this study]. Furthermore, replacing D1-Glu189 with Gln, Lys, or Arg might be expected to alter the midpoint potentials of the Mn cluster in all of its oxidation states because of the very different pK_A values of Glu, Gln, Arg, and Lys. In cytochrome *c* peroxidase, replacing His175 with Gln increased the midpoint potential of the heme iron by at least 75 mV (*118*). In cytochrome *c*, replacing Met80 with His or Cys decreased the midpoint potential of the heme iron by 230 and 600 mV, respectively (*119*). In cytochrome *c*-550 from *Thiobacillus versutus*, replacing Met100 with Lys decreased the midpoint potential of the heme iron by 330 mV (*116*). The rate of charge recombination between $Q_A^{\bullet-}$ and the S_2 state of the Mn cluster is determined by the rate of electron transfer from $Q_A^{\bullet-}$ to $P_{680}^{\bullet+}$ and by the equilibrium: $S_1\ P_{680}^{\bullet+} \leftrightarrow S_2\ P_{680}$ (*74*, *81*, *82*, *88*). An alteration of the S_2/S_1 midpoint potential would alter this equilibrium and, therefore, would alter the rate of charge recombination between $Q_A^{\bullet-}$ and the S_2 state of the Mn cluster. However, the charge recombination kinetics of D1-E189Q, D1-E189K, and D1-E189R cells closely resemble those of wild-type* cells [not shown, but see Figure 11 of ref (*37*)]. These data imply that D1-Glu189 has little influence on the S_2/S_1 midpoint potential. On the basis of these considerations, we conclude that D1-Glu189 is unlikely to ligate the Mn cluster in PSII, in agreement with our earlier analysis (*37*). However, a definitive conclusion will require more direct studies.

The multiline EPR signals of D1-E189Q PSII particles in the S_1 and S_2 states (Figures 4 and 5) closely resemble those observed in wild-type* PSII particles. These similarities provide additional, but not conclusive, evidence that D1-Glu189 does not ligate the Mn cluster. One might expect that replacing a carboxylate ligand with the corresponding carboxamide would alter the magnetic properties of the Mn cluster. However, the absence of such alterations in D1-E189Q PSII particles does not rigorously exclude D1-Glu189 as a ligand to the Mn cluster. As a possible counterexample, D1-Asp170 is most likely a ligand of the Mn cluster (*99*) [for review, see (*4*, *5*, *11*)], but D1-D170H PSII particles exhibit normal multiline EPR spectra in both the S_1 state (K. A. Campbell, R. D. Britt, and R. J. Debus, unpublished observations) and the S_2 state (X.-S. Tang and B. A. Diner, personal communication; K. A. Campbell, R. D. Britt, and R. J. Debus, unpublished observations). Nevertheless, we can exclude the possibility that D1-Glu189 acts as a bridging ligand between two Mn ions or as a bidentate ligand to a single Mn ion.

The absence of S_1 and S_2 state multiline EPR signals in the nonphotoautotrophic D1-Glu189 mutants shows that the magnetic properties of the Mn cluster are altered in these mutants. In these mutants, "split" EPR signals are accumulated under multiple turnover conditions (Figures 6 and 7). These signals resemble those observed in PSII preparations from spinach that have been depleted of Ca^{2+} (*20*, *21*, *120*−*124*) or Cl^- (*124*, *125*), or that have been treated with acetate (*13*, *17*−*20*, *22*, *107*−*111*, *126*) or NH_3 (*22*, *127*, *128*). The "split" EPR signals observed in the D1-Glu189 mutants are narrower than those observed in Ca^{2+}-depleted or acetate-treated PSII preparations from spinach, but are similar in width to those observed in Cl^--depleted (*124*) and NH_3-treated (*22*, *127*, *128*) PSII preparations from spinach and in Ca^{2+}-depleted PSII particles from *Synechocystis* sp. PCC 6803 (*129*), the organism used in the present study. Of particular note, the "split" EPR signal of D1-E189G PSII particles exhibits features (Figure 6B) that resemble the multiline peaks flanking the split EPR signal observed in acetate-treated preparations (*13*, *17*−*20*, *107*−*111*). Hints of such features are also evident in the D1-E189D, D1-E189N, and D1-E189S PSII particles (Figures 6B and 7).

Depletion of Ca^{2+}, depletion of Cl^-, and treatment with acetate all block advancement beyond the $Y_Z^{\bullet}S_2$ state (*25*, *109*, *126*). Treatment with NH_3 slows one or more of the S state transitions (*130*). In these inhibited preparations, the "split" EPR signal arises from a magnetic interaction between $Y_Z^{\bullet}$ and the S_2 state of the Mn cluster (*25*, *109*, *126*). The line shape of this signal is determined by the magnetic properties of the Mn cluster and by the relative orientation and distance between the Mn cluster and $Y_Z^{\bullet}$ (*13*, *17*−*20*, *111*). Therefore, the difference in line shapes between "split" EPR signals observed in different D1-Glu189 mutants must reflect differences in one or more of these parameters.

Because no S_2 state multiline EPR signal is observed in the nonphotoautotrophic D1-Glu189 mutants, we are unable to exclude the possibility that the "split" EPR signals observed in these mutants may arise from a magnetic interaction between $Y_Z^{\bullet}$ and a Mn cluster containing fewer than four Mn ions or having an oxidation state less than S_2. In principle, a "split" EPR signal with flanking multiline features could arise from a magnetic interaction between $Y_Z^{\bullet}$ and a paramagnetic Mn cluster having a nuclearity of 2 or higher, including the possibility of oxidation state differing from any of the known S states. However, no signals resembling the line shapes of known $Y_Z^{\bullet}S_2$ "split" EPR spectra have been reported in damaged wild-type PSII preparations, in PSII preparations containing fewer than four Mn ions [e.g., (*131*)], or in PSII preparations having Mn oxidation states lower than S_2 [e.g., (*132*)]. Furthermore, if Mn clusters having fewer than four Mn ions or dark-stable oxidation states lower than S_1 exist in the nonphotoautotrophic D1-Glu189 mutants, they are EPR-silent at X band both after dark-adaptation and after a single turnover (e.g., after illumination at 195 K or at 273 K in the presence of DCMU). Altered S_2 states that exhibit no multiline EPR signal have been reported previously. For example, no S_2 state multiline EPR signal was observed in PSII preparations from *Synechococcus elongatus* after illumination at 140 K and warming to 215 K despite X-ray absorption data showing that the Mn cluster had been oxidized at 140 K (*133*). Similarly, Cl^--depleted PSII preparations exhibit no S_2 state multiline EPR signal (*134*, *135*), and acetate-treated PSII preparations exhibit an S_2 state multiline EPR signal only under special circumstances (*109*, *111*). Consequently, our observation of "split" EPR signals in the nonphotoautotrophic D1-Glu189 mutants is consistent with an inability to advance beyond an altered $Y_Z^{\bullet}S_2$ state in these mutants. We favor this interpretation. An inability to advance beyond an altered $Y_Z^{\bullet}S_2$ state would be consistent with the inability of the

[6] Possible reasons for the retention of O_2 evolution and photoautotrophic growth in the D1-E189L and D1-E189I mutants are discussed below.

nonphotoautotrophic D1-Glu189 mutants to evolve O_2 and with the progressive quenching of the maximal yield of chlorophyll *a* fluorescence observed in intact cells of these mutants (e.g., Figure 1).

Few D1-E189G Mn clusters and only a minority of D1-E189S Mn clusters (43 ± 6%) reduce $Y_Z^•$ after a flash; the remaining Mn clusters protect $Y_Z^•$ from reduction by exogenous Mn^{2+} ions (Figure 2). A similar phenomenon was reported recently in D1-H332E PSII particles (*136*). As in this earlier study, we propose that the low quantum yield of oxidation of endogenous Mn clusters in D1-E189G and D1-E189S PSII particles is caused by a dramatic slowing of the rate of electron transfer from the Mn cluster to $Y_Z^•$ during the $S_1 \rightarrow S_2$ transition. In the D1-E189S PSII particles, the extent of slowing can be estimated. If only $Q_A^{•-}$ and the Mn cluster compete to reduce $Y_Z^•$ in these PSII particles, then, because $Q_A^{•-}$ reduces $Y_Z^•$ with $k^{-1} \approx 104$ ms (Table 2) and only 43 ± 6% of the Mn clusters in D1-E189S PSII particles reduce $Y_Z^•$ after a flash, the rate of electron transfer from Mn to $Y_Z^•$ during the $S_1 \rightarrow S_2$ transition must have $k^{-1} \approx 140$ ms. This rate constant is 1400-fold slower than that in wild-type PSII preparations, where $Y_Z^•$ oxidizes the S_1 state Mn cluster with a half-time of 55−110 μs (i.e., with $k^{-1} = 80-160$ μs) [(*75*−*78*) and references cited therein]. An 8000-fold slowing of this rate constant was estimated in D1-H332E PSII particles (*136*), and a even greater slowing may occur in D1-E189G PSII particles.

The low quantum yield for the oxidation of the Mn clusters in D1-E189S and D1-E189G PSII particles raises the possibility that the formation kinetics and stabilities of one or more intermediates formed during photoactivation of the Mn cluster [(*137*−*141*) and references cited therein] may be altered in these mutants. In contrast to the oxidation of assembled or partly assembled Mn clusters, the quantum yield for the oxidation of a single Mn^{2+} ion by $Y_Z^•$ appears to be normal in D1-E189S and D1-E189G PSII particles (Figure 2G,H).

The low quantum yield for oxidation of the Mn cluster in D1-E189G and D1-E189S PSII particles and the inability to advance beyond an apparent $Y_Z^•S_2$ state in D1-E189D, D1-E189G, D1-E189N, D1-E189S, and D1-E189H PSII particles show that the redox properties of the Mn cluster are altered dramatically in the nonphotoautotrophic D1-Glu189 mutants. The midpoint potential of Y_Z also appears to be altered in these mutants. In the absence of the Mn cluster, the rate of charge recombination between $Q_A^{•-}$ and $Y_Z^•$ is accelerated in D1-Glu189 mutant PSII particles compared to that in wild-type* PSII particles (Figure 3). As stated earlier, the rate of this reaction is determined by the rate of electron transfer from $Q_A^{•-}$ to $P_{680}^{•+}$ and by the equilibrium, $P_{680}^{•+}\ Y_Z \leftrightarrow P_{680}\ Y_Z^•$ (*74*, *80*−*82*, *88*, *93*). Although we are unable to exclude an alteration of the redox properties of Q_A or P_{680}, it seems more likely that the accelerated rate of charge recombination between $Q_A^{•-}$ and $Y_Z^•$ in Mn-depleted D1-Glu189 mutant PSII particles represents an alteration of the redox properties of Y_Z. The rate of charge recombination between $Q_A^{•-}$ and $Y_Z^•$ is significantly faster in Mn-depleted D1-E189D PSII particles than in all other D1-Glu189 mutant PSII particles (Figure 3). This finding is consistent with the ideas of David Kramer and co-workers, who propose that D1-His190 and D1-Glu189 interact via a hydrogen bond and that D1-His190 would bond more strongly with Asp189 than with Glu189 (*54*).

The dramatic differences in the O_2-evolving and fluorescence characteristics of D1-E189Q and D1-E189D cells previously led us to propose that D1-Glu189 participates in a network of hydrogen bonds that is crucial for positioning a residue that participates in proton release during water oxidation (*37*). More recently, this residue has been proposed to participate in a proton-transfer pathway leading from D1-His190 to the lumenal surface, and to accept a proton from D1-His190 either directly or by positioning a group that acts as a proton acceptor (*29*, *31*, *33*). Mutant D1-E189Q cells are photoautotrophic and evolve O_2 at ∼70% the rate of wild-type* cells. Therefore, if D1-Glu189 accepts a proton directly from D1-His190, then another group must also accept a hydrogen bond from D1-His190 and must readily substitute for D1-Glu189 in the D1-E189Q mutant. An alternate scenario is that D1-Glu189 participates in a network of hydrogen bonds that positions the proton acceptor for D1-His190. Such a hydrogen-bonded network could be maintained by Gln. There is a precedent for such a replacement of a carboxylate moiety by the corresponding carboxamide: in dihydrofolate reductase, a hydrogen bond network involving Asp-27 is retained in the D27N mutation because an O−HN hydrogen bond is simply replaced by an NH−N hydrogen bond (*142*). The flexibility and hydrogen-bonding properties of Lys and Arg may similarly permit these residues to maintain a network of hydrogen bonds in place of Glu189 (*143*), especially if the network involves water molecules, as seems likely in PSII on the basis of the hydrogen-bonded networks observed in bacterial reaction centers (*44*, *45*), bacteriorhodopsin (*46*−*48*), cytochrome *f* (*49*, *50*), and cytochrome *c* oxidase (*51*−*53*). None of the other residues substituted for D1-Glu189 would be likely candidates for maintaining such a network of hydrogen bonds. Both Asp and Asn are shorter and less flexible than Glu and Gln (*144*). Indeed, the substitution of Glu by Asp can be deleterious to function because the position and orientation of the carboxylate moiety necessarily change in the structure of the mutant protein [e.g., the E43D mutation in staphylococcal nuclease (*145*) and the E165D mutation in triosephosphate isomerase (*146*)]. Why, then, do the mutations D1-E189L and D1-E189I support O_2 evolution and photoautotrophic growth? One possibility is that Leu and Ile, being relatively bulky and hydrophobic, cause structural perturbations that permit the missing D1-Glu189 carboxylate moiety to be replaced by another residue or by a water molecule (*37*). Such compensatory, mutation-induced structural rearrangements have been observed in ferredoxin I of *Azotobacter vinelandii* (*147*), ricin A (*148*), and human alcohol dehydrogenase (*149*). Such compensatory structural rearrangements were proposed previously to account for the photoautotrophic growth of D1-D170L, D1-D170I, and D1-D170V cells (*37*) and to account for the curious observation that the substitution of D1-His337 with progressively bulkier and more hydrophobic residues causes progressively less perturbation to the Mn cluster: whereas the Mn clusters in D1-H337V cells are severely perturbed, those in D1-H337L cells evolve O_2 and those in D1-H337F cells support photoautotrophic growth (*79*).

That acetate-inhibited, Ca^{2+}-depleted, Cl^--depleted, and nonphotoautotrophic D1-Glu189 mutant PSII preparations

are all unable to advance beyond the $S_2Y_Z^\bullet$ state suggests a mechanism for the inhibition of Mn oxidation in the nonphotoautotrophic D1-Glu189 mutants. Both acetate-treatment (*92*, *150*) and Ca^{2+}-depletion (*124*, *151*) dramatically slow the oxidation of Y_Z by $P_{680}^{\bullet+}$. This phenomenon is also observed in D1-His190 mutants, where the hydrogen-bonding properties of Y_Z are disrupted (*34*−*41*). Consequently, both acetate-treatment and Ca^{2+}-depletion are believed to disrupt a network of hydrogen bonds that includes Y_Z and D1-His190 (*33*, *41*, *151*, *152*). To provide the necessary driving force for oxidizing the Mn cluster, $Y_Z^\bullet$ has been proposed to abstract both an electron and a proton from the Mn cluster in its S_2 and S_3 states (*5*, *14*, *23*−*26*, *28*−*33*, *109*). Acetate-treatment, Ca^{2+}-depletion, and Cl^--depletion all have been proposed to block the conversion of $S_2Y_Z^\bullet$ to S_3Y_Z by inhibiting proton transfer from Mn to $Y_Z^\bullet$: these treatments have been proposed to disrupt a network of hydrogen bonds that connects Y_Z with the water-derived Mn ligands from which the proton is abstracted (*24*, *33*, *109*, *152*). A similar disruption of these hydrogen bonds, or those connecting Y_Z and D1-His190 with proton-transfer pathways leading to the lumenal surface, may occur in the nonphotoautotrophic D1-Glu189 mutants.

ACKNOWLEDGMENT

We are grateful to G. T. Babcock, G. W. Brudvig, A. R. Crofts, D. M. Kramer, and F. Rappaport for helpful discussions, to A. P. Nguyen for maintaining the wild-type* and mutant cultures of *Synechocystis* 6803 and for help in isolating some of the PSII particles, and to the reviewers for helpful comments on the manuscript.

REFERENCES

1. Rhee, K. H., Morris, E. P., Barber, J., and Kühlbrandt, W. (1998) *Nature 396*, 283−286.
2. Hankamer, B., Morris, E. P., and Barber, J. (1999) *Nat. Struct. Biol. 6*, 560−564.
3. Nield, J., Orlova, E. V., Morris, E. P., Gowen, B., van Heel, M., and Barber, J. (2000) *Nat. Struct. Biol. 7*, 44−47.
4. Debus, R. J. (1992) *Biochim. Biophys. Acta 1102*, 269−352.
5. Britt, R. D. (1996) in *Oxygenic Photosynthesis: The Light Reactions* (Ort, D. R., and Yocum, C. F., Eds.) pp 137−164, Kluwer Academic Publishers, Dordrecht, The Netherlands.
6. Diner, B. A., and Babcock, G. T. (1996) in *Oxygenic Photosynthesis: The Light Reactions* (Ort, D. R., and Yocum, C. F., Eds.) pp 213−247, Kluwer Academic Publishers, Dordrecht, The Netherlands.
7. Yachandra, V. K., Sauer, K., and Klein, M. P. (1996) *Chem. Rev. 96*, 2927−2950.
8. Renger, G. (1997) *Physiol. Plant. 100*, 828−841.
9. Penner-Hahn, J. E. (1998) *Struct. Bonding 90*, 1−36.
10. Hoganson, C. W., and Babcock, G. T. (2000) in *Metal Ions in Biological Systems* (Sigel, A., and Sigel, H., Eds.) Vol. 37, pp 613−656, Marcel Dekker, New York.
11. Debus, R. J. (2000) in *Metal Ions in Biological Systems* (Sigel, A., and Sigel, H., Eds.) Vol. 37, pp 657−710, Marcel Dekker, New York.
12. Randall, D. W., Sturgeon, B. E., Ball, J. A., Lorigan, G. A., Chan, M. K., Klein, M. P., Armstrong, W. H., and Britt, R. D. (1995) *J. Am. Chem. Soc. 117*, 11780−11789.
13. Peloquin, J. M., Campbell, K. A., and Britt, R. D. (1998) *J. Am. Chem. Soc. 120*, 6840−6841.
14. Britt, R. D., Peloquin, J. M., and Campbell, K. A. (2000) *Annu. Rev. Biophys. Biomol. Struct.* (in press).
15. Roelofs, T. A., Liang, W., Latimer, M. J., Cinco, R. M., Rompel, A., Andrews, J. C., Sauer, K., Yachandra, V. K., and Klein, M. P. (1996) *Proc. Natl. Acad. Sci. U.S.A. 93*, 3335−3340.
16. Iuzzolino, L., Dittmer, J., Dörner, W., Meyer-Klaucke, W., and Dau, H. (1998) *Biochemistry 37*, 17112−17119.
17. Dorlet, P., Di Valentin, M., Babcock, G. T., and McCracken, J. L. (1998) *J. Phys. Chem. B 102*, 8239−8247.
18. Lakshmi, K. V., Eaton, S. S., Eaton, G. R., Frank, H. A., and Brudvig, G. W. (1998) *J. Phys. Chem. B 102*, 8327−8335.
19. Lakshmi, K. V., Eaton, S. S., Eaton, G. R., and Brudvig, G. W. (1999) *Biochemistry 38*, 12758−12767.
20. Dorlet, P., Boussac, A., Rutherford, A. W., and Un, S. (1999) *J. Phys. Chem. B 103*, 10945−10954.
21. Boussac, A., Zimmermann, J.-L., Rutherford, A. W., and Lavergne, J. (1990) *Nature 347*, 303−306.
22. MacLachlan, D. J., Nugent, J. H. A., Warden, J. T., and Evans, M. C. W. (1994) *Biochim. Biophys. Acta 1188*, 325−334.
23. Tommos, C., Hoganson, C. W., Di Valentin, M., Lydakis-Simantiris, N., Dorlet, P., Westphal, K., Chu, H.-A., McCracken, J., and Babcock, G. T. (1998) *Curr. Opin. Chem. Biol. 2*, 244−252.
24. Limburg, J., Szalai, V. A., and Brudvig, G. W. (1999) *J. Chem. Soc., Dalton Trans.*, 1353−1361.
25. Gilchrist, M. L., Jr., Ball, J. A., Randall, D. W., and Britt, R. D. (1995) *Proc. Natl. Acad. Sci. U.S.A. 92*, 9545−9549.
26. Pecoraro, V. L., Baldwin, J. M., Caudle, M. T., Hsich, W.-Y., and Law, N. A. (1998) *Pure Appl. Chem. 70*, 925−929.
27. Haumann, M., and Junge, W. (1999) *Biochim. Biophys. Acta 1411*, 86−91.
28. Hoganson, C. W., Lydakis-Simantiris, N., Tang, X.-S., Tommos, C., Warncke, K., Babcock, G. T., Diner, B. A., McCracken, J., and Styring, S. (1995) *Photosynth. Res. 46*, 177−184.
29. Babcock, G. T. (1995) in *Photosynthesis: From Light to Biosphere* (Mathis, P., Ed.) Vol. II, pp 209−215, Kluwer Academic Publishers, Dordrecht.
30. Hoganson, C. W., and Babcock, G. T. (1997) *Science 277*, 1953−1956.
31. Tommos, C., and Babcock, G. T. (1998) *Acc. Chem. Res. 31*, 18−25.
32. Siegbahn, P. E., and Crabtree, R. H. (1999) *J. Am. Chem. Soc. 121*, 117−127.
33. Tommos, C., and Babcock, G. T. (2000) *Biochim. Biophys. Acta* (in press).
34. Diner, B. A., Nixon, P. J., and Farchaus, J. W. (1991) *Curr. Opin. Struct. Biol. 1*, 546−554.
35. Roffey, R. A., Kramer, D. M., Govindjee, and Sayre, R. T. (1994) *Biochim. Biophys. Acta 1185*, 257−270.
36. Roffey, R. A., van Wijk, K. J., Sayre, R. T., and Styring, S. (1994) *J. Biol. Chem. 269*, 5115−5121.
37. Chu, H.-A., Nguyen, A. P., and Debus, R. J. (1995) *Biochemistry 34*, 5839−5858.
38. Mamedov, F., Sayre, R. T., and Styring, S. (1998) *Biochemistry 37*, 14245−14256.
39. Hays, A.-M. A., Vassiliev, I. R., Golbeck, J. H., and Debus, R. J. (1998) *Biochemistry 37*, 11352−11365.
40. Diner, B. A., and Nixon, P. J. (1998) in *Photosynthesis: Mechanisms and Effects* (Garab, G., Ed.) Vol. II, pp 1177−1180, Kluwer Academic Publishers, Dordrecht, The Netherlands.
41. Hays, A.-M. A., Vassiliev, I. R., Golbeck, J. H., and Debus, R. J. (1999) *Biochemistry 38*, 11851−11865.
42. Nagle, J. F., and Tristram-Nagle, S. (1983) *J. Membr. Biol. 74*, 1−14.
43. Pomès, R., and Roux, B. (1996) *J. Phys. Chem. 100*, 2519−2527.
44. Abresch, E. C., Paddock, M. L., Stowell, M. H., McPhillips, T. M., Axelrod, H. L., Soltis, S. M., Rees, D. C., Okamura, M. Y., and Feher, G. (1998) *Photosynth. Res. 55*, 119−125.
45. Fritzsch, G., Kampmann, L., Kapaun, G., and Michel, H. (1998) *Photosynth. Res. 55*, 127−132.
46. Luecke, H., Richter, H. T., and Lanyi, J. K. (1998) *Science 280*, 1934−1937.

47. Belrhali, H., Nollert, P., Royant, A., Menzel, C., Rosenbusch, J. P., Landau, E. M., and Pebay-Peyroula, E. (1999) *Structure 7*, 909−917.
48. Luecke, H., Schobert, B., Richter, H.-T., Cartailler, J. P., and Lanyi, J. K. (1999) *J. Mol. Biol. 291*, 899−911.
49. Martinez, S. E., Huang, D., Ponomarev, M., Cramer, W. A., and Smith, M. (1996) *Protein Sci. 5*, 1081−1092.
50. Carrell, C. J., Schlarb, B. G., Bendall, D. S., Howe, C. J., Cramer, W. A., and Smith, J. L. (1999) *Biochemistry 38*, 9590−9599.
51. Tsukihara, T., Aoyama, H., Yamashita, E., Tomizaki, T., Yamaguchi, H., Shinzawa-Itoh, K., Nakashima, R., and Yoshikawa, S. (1996) *Science 272*, 1136−1144.
52. Ostermeier, C., Harrenga, A., Ermler, U., and Michel, H. (1997) *Proc. Natl. Acad. Sci. U.S.A. 94*, 10547−10553.
53. Yoshikawa, S., Shinzawa-Itoh, K., Nakashima, R., Yaono, R., Yamashita, E., Inoue, N., Yao, M., Fei, M. J., Peters Libeu, C., Mizushima, T., Yamaguchi, H., Tomizaki, T., and Tsukihara, T. (1998) *Science 280*, 1723−1729.
54. Kanazawa, A., Roberts, A., and Kramer, D. M. (1998) Seventh Western Regional Photosynthesis Conference, Pacific Grove, CA, Jan 8−11, 1998, Abstract 4−7.
55. Haumann, M., Mulkidjanian, A., and Junge, W. (1999) *Biochemistry 38*, 1258−1267.
56. Svensson, B., Vass, I., and Styring, S. (1991) *Z. Naturforsch. 46C*, 765−776.
57. Ruffle, S. V., Donnelly, D., Blundell, T. L., and Nugent, J. H. A. (1992) *Photosynth. Res. 34*, 287−300.
58. Svensson, B., Etchebest, C., Tuffery, P., Van Kan, P., Smith, J., and Styring, S. (1996) *Biochemistry 35*, 14486-14502.
59. Xiong, J., Subramaniam, S., and Govindjee (1998) *Photosynth. Res. 56*, 229−254.
60. Debus, R. J., Campbell, K. A., Pham, D. P., Hays, A.-M. A., Peloquin, J. M., and Britt, R. D. (1998) in *Photosynthesis: Mechanisms and Effects* (Garab, G., Ed.) Vol. II, pp 1375−1378, Kluwer Academic Publishers, Dordrecht, The Netherlands.
61. Chu, H.-A., Nguyen, A. P., and Debus, R. J. (1994) *Biochemistry 33*, 6137−6149.
62. Debus, R. J., Nguyen, A. P., and Conway, A. B. (1990) in *Current Research in Photosynthesis* (Baltscheffsky, M., Ed.) Vol. I, pp 829−832, Kluwer Academic Publishers, Dordrecht.
63. Chu, H.-A., Nguyen, A. P., and Debus, R. J. (1995) in *Photosynthesis: From Light to Biosphere* (Mathis, P., Ed.) Vol. II, pp 439−442, Kluwer Academic Publishers, Dordrecht, The Netherlands.
64. Williams, J. G. K. (1988) *Methods Enzymol. 167*, 766−778.
65. Vermaas, W. F. J. (1994) *Biochim. Biophys. Acta 1187*, 181−186.
66. Tang, X.-S., and Diner, B. A. (1994) *Biochemistry 33*, 4594−4603.
67. Tang, X.-S., Zheng, M., Chisholm, D. A., Dismukes, G. C., and Diner, B. A. (1996) *Biochemistry 35*, 1475−1484.
68. Lichtenthaler, H. K. (1987) *Methods Enzymol. 148*, 350−382.
69. Wingo, W. J., and Emerson, G. M. (1975) *Anal. Chem. 47*, 351−352.
70. Krause, G. H., and Weis, E. (1991) *Annu. Rev. Plant Physiol. Plant Mol. Biol. 42*, 313−349.
71. Holzwarth, A. R. (1991) in *Chlorophylls* (Scheer, H., Ed.) pp 1125−1151, CRC Press, Boca Raton, FL.
72. Dau, H. (1994) *Photochem. Photobiol. 60*, 1−23.
73. Nixon, P. J., and Diner, B. A. (1992) *Biochemistry 31*, 942−948.
74. Diner, B. A. (1998) *Methods Enzymol. 297*, 337−360.
75. van Leeuwen, P. J., Heimann, C., Gast, P., Dekker, J. P., and van Gorkom, H. J. (1993) *Photosynth. Res. 38*, 169−176.
76. Rappaport, F., Blanchard-Desce, M., and Lavergne, J. (1994) *Biochim. Biophys. Acta 1184*, 178−192.
77. Razeghifard, M. R., Klughammer, C., and Pace, R. J. (1997) *Biochemistry 36*, 86−92.
78. Razeghifard, M. R., and Pace, R. J. (1997) *Biochim. Biophys. Acta 1322*, 141−150.
79. Chu, H.-A., Nguyen, A. P., and Debus, R. J. (1995) *Biochemistry 34*, 5859−5882.
80. Buser, C. A., Thompson, L. K., Diner, B. A., and Brudvig, G. W. (1990) *Biochemistry 29*, 8977−8985.
81. Vass, I., and Styring, S. (1991) *Biochemistry 30*, 830−839.
82. Buser, C. A., Diner, B. A., and Brudvig, G. W. (1992) *Biochemistry 31*, 11449−11459.
83. Stewart, D. H., and Brudvig, G. W. (1998) *Biochim. Biophys. Acta 1367*, 63−87.
84. Thompson, L. K., and Brudvig, G. W. (1988) *Biochemistry 27*, 6653−6658.
85. Stewart, D. H., Cua, A., Chisholm, D. A., Diner, B. A., Bocian, D. F., and Brudvig, G. W. (1998) *Biochemistry 37*, 10040−10046.
86. Hanley, J., Deligiannakis, Y., Pascal, A. A., Faller, P., and Rutherford, A. W. (1999) *Biochemistry 38*, 8189−8195.
87. Vrettos, J. S., Stewart, D. H., de Paula, J. C., and Brudvig, G. W. (1999) *J. Phys. Chem. B 103*, 6403−6406.
88. Buser, C. A. (1993) Ph.D. Dissertation, Yale University, New Haven, CT.
89. van Gorkom, H. J. (1974) *Biochim. Biophys. Acta 347*, 439−442.
90. Dekker, J. P., van Gorkom, H. J., Brok, M., and Ouwehand, L. (1984) *Biochim. Biophys. Acta 764*, 301−309.
91. Schatz, G. H., and van Gorkom, H. J. (1985) *Biochim. Biophys. Acta 810*, 283−294.
92. Gerken, S., Dekker, J. P., Schlodder, E., and Witt, H. T. (1989) *Biochim. Biophys. Acta 977*, 52−61.
93. Metz, J. G., Nixon, P. J., Rögner, M., Brudvig, G. W., and Diner, B. A. (1989) *Biochemistry 28*, 6960−6969.
94. Rappaport, F., and Lavergne, J. (1997) *Biochemistry 36*, 15294−15302.
95. Hoganson, C. W., Ghanotakis, D. F., Babcock, G. T., and Yocum, C. F. (1989) *Photosynth. Res. 22*, 285−293.
96. Diner, B. A., and Nixon, P. J. (1992) *Biochim. Biophys. Acta 1101*, 134−138.
97. Magnuson, A., and Andréasson, L.-E. (1997) *Biochemistry 36*, 3254−3261.
98. Ono, T.-A., and Mino, H. (1999) *Biochemistry 38*, 8778−8785.
99. Campbell, K. A., Force, D. A., Nixon, P. J., Dole, F., Diner, B. A., and Britt, R. D. (2000) *J. Am. Chem. Soc. 122*, 3754−3761.
100. Lavergne, J., and Rappaport, F. (1998) *Biochemistry 37*, 7899−7906.
101. Boerner, R. J., Nguyen, A. P., Barry, B. A., and Debus, R. J. (1992) *Biochemistry 31*, 6660−6672.
102. Brettel, K., Schlodder, E., and Witt, H. T. (1984) *Biochim. Biophys. Acta 766*, 403−415.
103. Ahlbrink, R., Haumann, M., Cherepanov, D., Bögershausen, O., Mulkidjanian, A., and Junge, W. (1998) *Biochemistry 37*, 1131−1142.
104. Yerkes, C. T., Babcock, G. T., and Crofts, A. R. (1983) *FEBS Lett. 158*, 359−363.
105. Campbell, K. A., Peloquin, J. M., Pham, D. P., Debus, R. J., and Britt, R. D. (1998) *J. Am. Chem. Soc. 120*, 447−448.
106. Campbell, K. A., Gregor, W., Pham, D. P., Peloquin, J. M., Debus, R. J., and Britt, R. D. (1998) *Biochemistry 37*, 5039−5045.
107. MacLachlan, D. J., and Nugent, J. H. A. (1993) *Biochemistry 32*, 9772−9780.
108. Szalai, V. A., and Brudvig, G. W. (1996) *Biochemistry 35*, 1946−1953.
109. Szalai, V. A., and Brudvig, G. W. (1996) *Biochemistry 35*, 15080−15087.
110. Force, D. A., Randall, D. W., and Britt, R. D. (1997) *Biochemistry 36*, 12062−12070.
111. Szalai, V. A., Kühne, H., Lakshmi, K. V., and Brudvig, G. W. (1998) *Biochemistry 37*, 13594−13603.
112. Ferrer, J. C., Guillemette, J. G., Bogumil, R., Inglis, S. C., Smith, M., and Mauk, A. G. (1993) *J. Am. Chem. Soc. 115*, 7507−7508.
113. Hampsey, D. M., Das, G., and Sherman, F. (1986) *J. Biol. Chem. 261*, 3259−3271.
114. Sorrell, T. N., Martin, P. K., and Bowden, E. F. (1989) *J. Am. Chem. Soc. 111*, 766−767.

115. Garcia, L. L., Fredericks, Z., Sorrell, T. N., and Pielack, G. J. (1992) *New J. Chem. 16*, 629−632.
116. Ubbink, M., Campos, A. P., Teixeira, M., Hunt, N. I., Hill, H. A. O., and Canters, G. W. (1994) *Biochemistry 33*, 10051−10059.
117. Sundaramoorthy, M., Choudhury, K., Edwards, S. L., and Poulos, T. L. (1991) *J. Am. Chem. Soc. 113*, 7755−7757.
118. Choudhury, K., Sundaramoorthy, M., Hickman, A., Yonetani, T., Woehl, E., Dunn, M. F., and Poulos, T. L. (1994) *J. Biol. Chem. 269*, 20239−20249.
119. Raphael, A. L., and Gray, H. B. (1991) *J. Am. Chem. Soc. 113*, 1038−1040.
120. Boussac, A., Zimmermann, J.-L., and Rutherford, A. W. (1989) *Biochemistry 28*, 8984−8989.
121. Sivaraja, M., Tso, J., and Dismukes, G. C. (1989) *Biochemistry 28*, 9459−9464.
122. Ono, T.-A., and Inoue, Y. (1990) *Biochim. Biophys. Acta 1020*, 269−277.
123. Boussac, A., Zimmermann, J.-L., and Rutherford, A. W. (1990) *FEBS Lett. 277*, 69−74.
124. Boussac, A., Sétif, P., and Rutherford, A. W. (1992) *Biochemistry 31*, 1224−1234.
125. Baumgarten, M., Philo, J. S., and Dismukes, G. C. (1990) *Biochemistry 29*, 10814−10822.
126. Tang, X.-S., Randall, D. W., Force, D. A., Diner, B. A., and Britt, R. D. (1996) *J. Am. Chem. Soc. 118*, 7638−7639.
127. Andréasson, L.-E., and Lindberg, K. (1992) *Biochim. Biophys. Acta 1100*, 177−183.
128. Hallahan, B. J., Nugent, J. H. A., Warden, J. T., and Evans, M. C. W. (1992) *Biochemistry 31*, 4562−4573.
129. Kirilovsky, D. L., Boussac, A. G. P., van Mieghem, F. J. E., Ducruet, J.-M. R. C., Sétif, P. R., Yu, J., Vermaas, W. F. J., and Rutherford, A. W. (1992) *Biochemistry 31*, 2099−2107.
130. Boussac, A., Rutherford, A. W., and Styring, S. (1990) *Biochemistry 29*, 24−32.
131. Ananyev, G. M., and Dismukes, G. C. (1997) *Biochemistry 36*, 11342−11350.
132. Ioannidis, N., Sarrou, J., Schansker, G., and Petrouleas, V. (1998) *Biochemistry 37*, 16445−16451.
133. McDermott, A. E., Yachandra, V. K., Guiles, R. D., Cole, J. L., Dexheimer, S. L., Britt, R. D., Sauer, K., and Klein, M. P. (1988) *Biochemistry 27*, 4021−4031.
134. Ono, T.-A., Zimmermann, J.-L., Inoue, Y., and Rutherford, A. W. (1986) *Biochim. Biophys. Acta 851*, 193−201.
135. Ono, T.-A., Nakayama, H., Gleiter, H., Inoue, Y., and Kawamori, A. (1987) *Arch. Biochem. Biophys. 256*, 618−624.
136. Debus, R. J., Campbell, K. A., Peloquin, J. M., Pham, D. P., and Britt, R. D. (2000) *Biochemistry 39*, 470−478.
137. Chen, C., Kazimir, J., and Cheniae, G. M. (1995) *Biochemistry 34*, 13511−13526.
138. Burnap, R. L., Qian, M., and Pierce, C. (1996) *Biochemistry 35*, 874−882.
139. Ananyev, G. M., and Dismukes, G. C. (1996) *Biochemistry 35*, 4102−4109.
140. Ananyev, G. M., and Dismukes, G. C. (1996) *Biochemistry 35*, 14608−14617.
141. Zaltsman, L., Ananyev, G. M., Bruntrager, E., and Dismukes, G. C. (1997) *Biochemistry 36*, 8914−8922.
142. Howell, E. E., Villafranca, J. E., Warren, M. S., Oatley, S. J., and Kraut, J. (1986) *Science 231*, 1123−1128.
143. Shimonik, L., and Glusker, J. P. (1995) *Protein Sci. 4*, 65−74.
144. Richardson, J. S., and Richardson, D. C. (1989) in *Prediction of Protein Structure and the Principles of Protein Conformation* (Fasman, G. D., Ed.) pp 1−98, Plenum Press, New York.
145. Loll, P. J., and Lattman, E. E. (1990) *Biochemistry 29*, 6866−6873.
146. Joseph-McCarthy, D., Rost, L. E., Komives, E. A., and Petsko, G. A. (1994) *Biochemistry 33*, 2824−2829.
147. Martín, A. E., Burgess, B. K., Stout, C. D., Cash, V. L., Dean, D. R., Jensen, G. M., and Stephens, P. M. (1990) *Proc. Natl. Acad. Sci. U.S.A. 87*, 598−602.
148. Kim, Y., Misna, D., Monzingo, A. F., Ready, M. P., Frankel, A., and Robertus, J. D. (1992) *Biochemistry 31*, 3294−3296.
149. Stone, C. L., Hurley, T. D., Amzel, L. M., Dunn, M. F., and Bosron, W. F. (1993) in *Enzymology and Molecular Biology of Carbonyl Metabolism 4* (Weiner, H., Ed.) pp 429−437, Plenum Press, New York.
150. Saygin, Ö., Gerken, S., Meyer, B., and Witt, H. T. (1986) *Photosynth. Res. 9*, 71−78.
151. Haumann, M., and Junge, W. (1999) *Biochim. Biophys. Acta 1411*, 121−133.
152. Tommos, C., McCracken, J., Styring, S., and Babcock, G. T. (1998) *J. Am. Chem. Soc. 120*, 10441−10452.

BI992749W